JOURNAL OF MATERIALS SCIENCE 25 (1990) 706–712

Tensile properties and fracture behaviour of polypropylene–nickel-coated carbon-fibre composite

V. DI LIELLO, E. MARTUSCELLI, G. RAGOSTA, A. ZIHLIF*
Istituto di Ricerche su Tecnologia dei Polimeri e Reologia, C.N.R., Via Toiano 6, 80072 Arco Felice, Napoli, Italy

Polypropylene-based composites reinforced with nickel-coated carbon fibres have been prepared and the effect of filler content on tensile properties and fracture behaviour at different temperatures and strain rates was investigated. The elastic modulus of such composites is enhanced by two orders of magnitude while the tensile strength and strain-to-break are lowered. The fracture toughness parameters, G_c and K_c, are also enhanced with filler content. The yield stress of this composite showed strain rate and temperature dependence. Activation energy and volume of a single rate-activated yielding process, at relatively high strain rates, were determined. The variations of the measured physical quantities are discussed in terms of the observed composite morphology.

1. Introduction

Polymer-based composites are recent products which play an essential role in many engineering and technological applications. The most common important example is the fibre-reinforced composites consisting of a polymer as a base (matrix) and glass, steel or carbon fibres as a filler. The structural design for use of this type of composites requires that they must have good durability and technical performance to withstand their use in various environmental conditions of temperature, pressure and weathering [1–6]. Thermoplastic polymers such as polypropylene are often reinforced by high-performance fibres in order to increase their stiffness, tensile strength and toughness. Recently, treated and coated short and long fibres have been used to improve the electrical performance of the engineering composites [7–11]. In the present study, we report the results of an investigation concerning the correlation between tensile properties and fracture behaviour of polypropylene–nickel-coated carbon-fibre composites with composition and SEM morphology. These results are part of a more general and comprehensive study having, as the main goal on the one side that of realizing new advanced composites characterized by both high mechanical properties and improved electrical and electromagnetic performance, and from the other side that of correlating between them factors such as fibre structure and type of coating, matrix structure, fibre–matrix adhesion and molecular and physical structure of interface regions.

2. Experimental details

2.1. Material and specimen preparation

The composite components used in the present study were isotatic polypropylene ($\bar{M}_n = 4.4 \times 10^5$, $\bar{M}_w = 1.0 \times 10^5$, $\bar{M}_w/\bar{M}_n = 4.4$); and nickel-coated carbon fibres of average measured diameter 10 μm, Young's modulus 80 GPa, and tensile strength 1.5 GPa. Fibre strands were provided by MARBO S.p.A. (Milan, Italy). They were chopped into single filaments of average length 1 mm and mixed with the polypropylene (matrix) using a brabender-like apparatus (Rheocord EC of Haake Inc.) operating at 200° C. This procedure was then followed by hot compression moulding at 200° C. The plates of composite obtained have thicknesses of 4 and 1.3 mm. The carbon fibre contents in these composites were 5, 10, 16 and 28 wt %.

2.2. Tensile tests

To study the deformation behaviour of these composite materials, dumb-bell specimens were cut from the 1.3 mm sheets. Tension tests were performed on an Instron testing machine equipped with an environmental chamber for work at different temperatures and over a range of strain rates. Temperature readings were taken by placing a thermometer near the test specimen.

2.3. Impact fracture tests

Fracture tests were carried out on a Charpy Instrumented Pendulum (Ceast Autographic Pendulum MK2), at an impact speed of 1 m sec^{-1}. Samples with a notch depth to width ratio of 0.3 and a test span of 48 mm were fractured at room temperature for all composite concentrations and at −80 to 20° C for 16 wt % carbon polypropylene composite. The relative curves of energy and load against time as displacement were recorded at each temperature.

*On sabbatical leave from the Physics Department, University of Jordan, Amman, Jordan.

0022–2461/90 $03.00 + .12

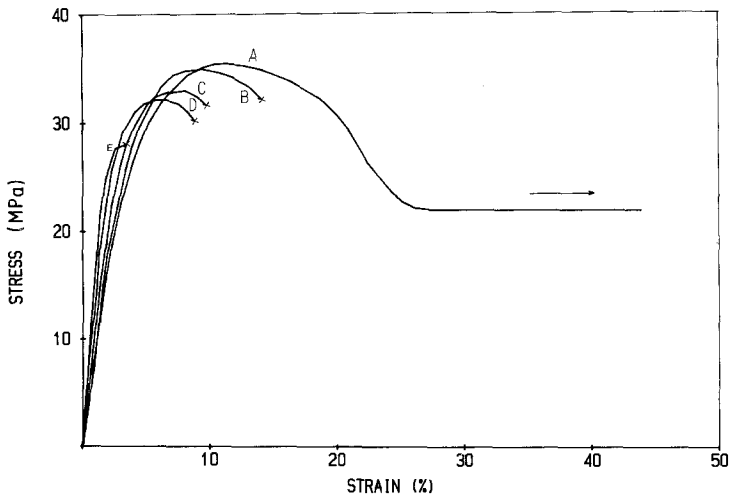

Figure 1 Typical stress–strain curves for carbon-fibre composites: (A) pure polypropylene; (B) 5 wt % fibres; (C) 10 wt % fibres; (D) 16 wt % fibres; (E) 28 wt % fibres. $\dot{\varepsilon} = 7.6 \times 10^{-3}\ \text{sec}^{-1}$.

2.4. Microscopy and X-ray diffraction

Adhesion and morphological investigations were carried out using a Philips 501 SEM on fracture surfaces obtained by tensile and impact tests. The samples for SEM observations were metal-coated using a Polaron sputtering apparatus with Au–Pd alloy. Optical examinations were carried out using a Wild M420 Stereomicroscope. The obtained X-ray diffraction patterns from the polypropylene (PP) matrix were concentric rings indicating isotropy. Thus no orientation of the matrix takes place during compression mouldings.

3. Results and discussion

3.1. Tensile results

Typical stress–strain curves corresponding to composite specimens of different fibre weight fractions and at a strain rate ($\dot{\varepsilon}$) $7.6 \times 10^{-3}\ \text{sec}^{-1}$ are shown by Fig. 1. Curve A for isotatic polypropylene represents a ductile plastic deformation behaviour. Curves B, C, D and E for 5, 10, 16 and 28 wt % fraction of fibres, respectively, show a much less ductile behaviour. It is clearly seen that brittleness increases with increasing fibre content and the composite becomes appreciably brittle at fibre concentration higher than 30% by weight. The ductile–brittle transition, is due to the brittleness of the carbon fibres embedded in the ductile PP matrix. The dependence of Young's modulus, calculated from the stress–strain curves, on the carbon-fibre content is shown in Fig. 2. The stiffness of the material increases linearly with weight fraction of the carbon fibres. This enhancement is expected, as it occurs for most polymers reinforced by high-performance fibres [1–3].

Fig. 3 shows the variations of tensile strength as a function of carbon fibre content. The strength decreases linearly with increasing carbon-fibre content. We believe that the observed decrease of the tensile strength with carbon-fibre content is caused by the brittle behaviour of the composites and not by the interfacial weakness between the fibres and matrix, as will be later seen from the morphological characteristics of the composites. Analogous to the tensile strength, the strain at break decreases with increasing the carbon-fibre content but, as shown by Fig. 4, the trends seem to be non-linear.

The yield stress was determined from the intersection of two tangents on the stress–strain curve for a ductile behaviour and from the maximum point for the brittle one. The calculated ratio of the yield stress to Young's modulus (σ_y/E) of the composites is plotted as a function of the carbon content in Fig. 5. The average values observed are found to be close to those of typical polymers and composites [4, 12]. As shown, σ_y/E decreases with carbon-fibre content. Such behaviour is accounted for by assuming that the yield stress decreases with fibre content not as rapidly as the elastic modulus increases.

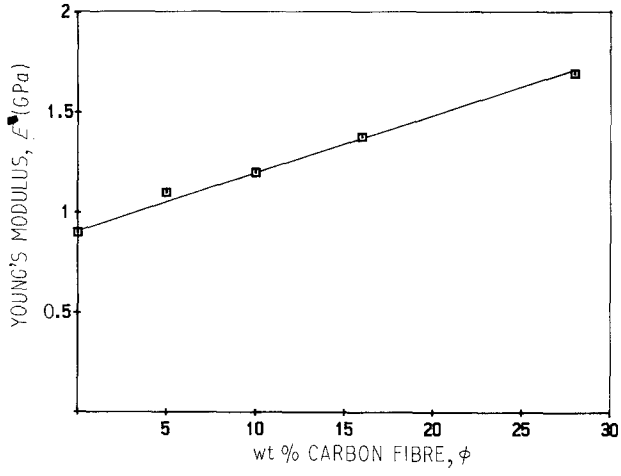

Figure 2 Youngs modulus of carbon-fibre reinforced polypropylene as a function of fibre content.

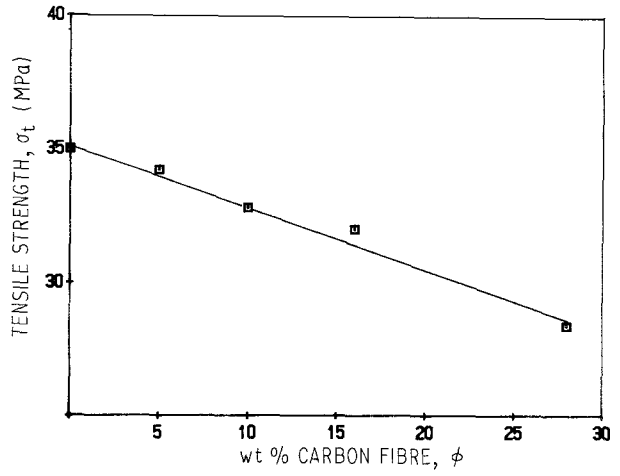

Figure 3 Tensile strength of polypropylene–carbon-fibre composite as a function of fibre content.

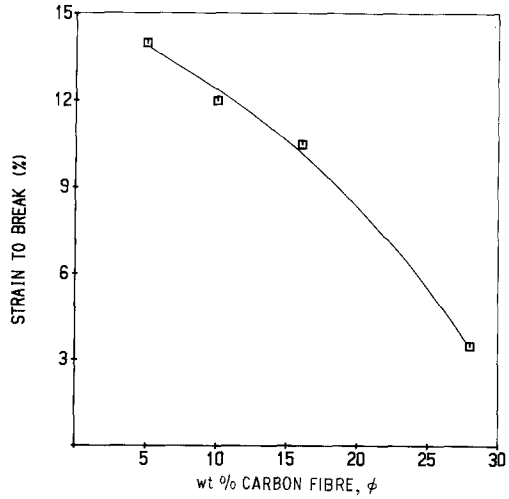

Figure 4 Dependence of the strain to break on carbon-fibre content for PP/carbon fibre composite.

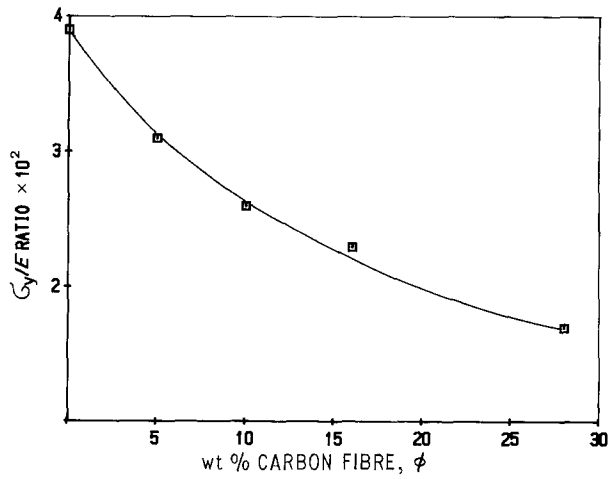

Figure 5 Yield stress/Youngs modulus ratio as a function carbon-fibre content.

Stress–strain curves were also obtained at different temperatures and strain rates. The tensile yield stress and Young's modulus for the 10 wt % composite measured over a temperature range from room temperature to 110° C are shown in Fig. 6. Both decrease nearly at the same rate with increasing temperature. The tensile yield stress for isotatic PP, 10 and 28 wt % specimens measured at room temperature is plotted as a function of log strain rate in Fig. 7. The data show a linear relationship between the yield stress and the strain rate for the PP polymer and the composites; but the straight lines are not parallel which indicates the occurrence of more than a single activated-rate process. This departure from parallelity is accounted for by the existence of the coated carbon fibres which possess a semiconductive behaviour [13] as filler elements. However, the data still show that the yield stress increases as a function of strain rate for the given composite. The equivalence between increasing yield stress and increasing strain rate and decreasing temperature can be drawn from Figs 6 and 7. The overall effect of the strain rate on yielding behaviour, shown in Fig. 7, can be described by the Eyring theory [14, 15]. The values of activation energy and stress activation volume are calculated using the Eyring equation for an activated-rate process, which can be written in terms of the strain rate, $\dot{\varepsilon}$, and absolute temperature, T, as

$$\dot{\varepsilon} = \dot{\varepsilon}_0 \exp\left[-(E_a - \sigma_y V^*)\right]/kT \quad (1)$$

where $\dot{\varepsilon}_0$ is constant, E_a is the activation energy for an activated-rate process, σ_y is the yield stress, V^* is the stress activation volume, k is Boltzmann constant, and T is the absolute temperature. This equation implies that the stress at yield and the logarithm of strain rate have a linear relationship with the slope given by

$$\partial\sigma_y/(\partial \ln \dot{\varepsilon})_T = kT/V^* \quad (2)$$

Values for the activation energy and the activation volume are calculated from the observed linear dependence of Fig. 7 for PP polymer and the other two composites. Fig. 8 shows the variations of activation energy, E_a, and the volume, V^*, as a function of weight fraction of coated carbon fibres. E_a decreases with the carbon-fibre content, while V^* increases. This observed dependence of E_a and V^* is attributed to the addition of the coated carbon-fibres (discussed later in Section 4). Recently, the effect of filler content on activation energy was reported [16, 17] for particulate-filled composites such as polypropylene filled with ultrafine particles and polybutadine filled with clay.

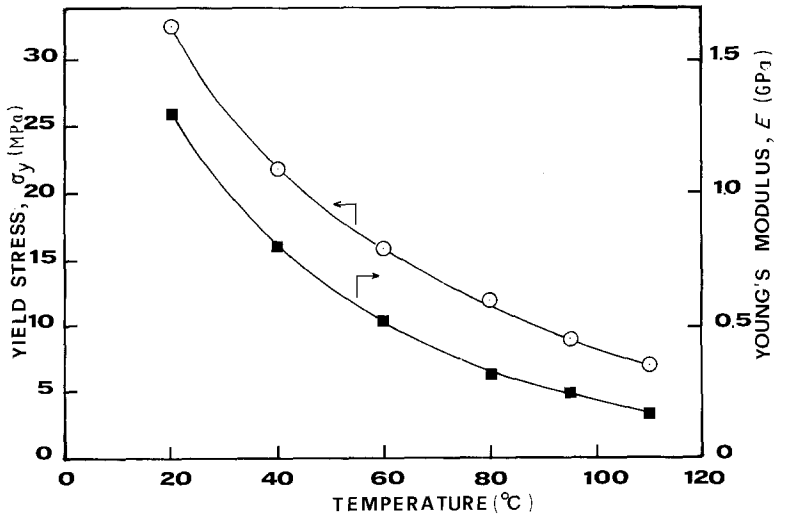

Figure 6 Variation of yield stress and Youngs modulus with temperature for 10 wt % carbon-fibre compose; $\dot{\varepsilon} = 7.6 \times 10^{-3}$ sec^{-1}.

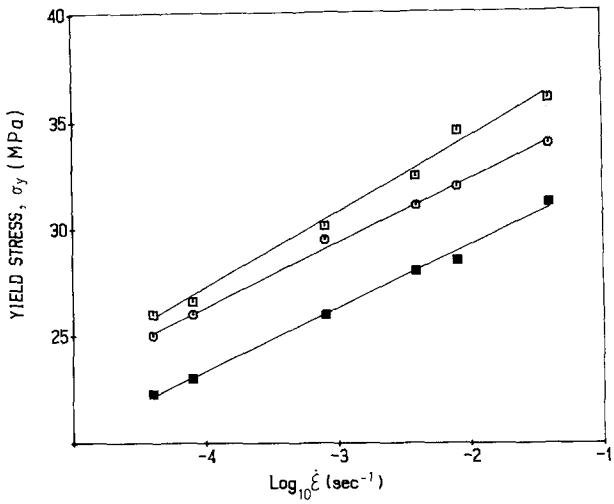

Figure 7 Dependence of the yield stress on strain rate for specimens of (□) pure polypropylene, (○) 10 wt % fibre composite and (■) 28 wt % fibre composite, tested at room temperature.

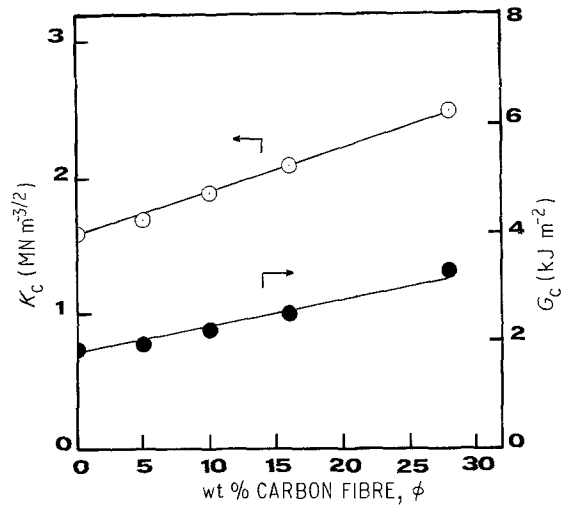

Figure 9 Critical stress intensity factor (K_c) and critical strain energy release rate (G_c) as a function of carbon-fibre content.

3.2. Impact fracture results

3.2.1. Fracture toughness parameters

The critical stress intensity factor, K_c, is calculated using the fracture mechanics approach [18, 19] from the equation

$$K_c = \sigma Y(a)^{1/2} \quad (3)$$

where σ is the nominal stress at the onset of crack propagation, a is the initial crack length and Y is a calibration factor depending on the specimen geometry.

For the determination of the critical strain energy release rate, G_c, the following equation is used

$$G_c = U/BW\phi \quad (4)$$

where U is the fracture energy corrected from the kinetic energy contribution, B and W are the thickness and the width of the specimen, respectively, and ϕ is a calibration factor which depends on the length of crack and size of the sample. The values of ϕ were taken from Plati and Williams [20].

3.2.2. Fracture toughness results

The critical strain energy release rate (G_c) as a function of coated carbon-fibre content at room temperature is shown in Fig. 9. The relationship between G_c and ϕ is a linear one, where the critical strain energy release rate increases with increasing fibre content. The enhancement of G_c observed at room temperature is mainly attributed to the occurrence of stiff localized aggregates of carbon fibres interacted with magnetic forces and to the existence of entanglement network between the fibres themselves and the PP matrix. These features of carbon fibres are able to toughen the composites structure. A similar behaviour is observed for the critical stress intensity factor, K_c.

Fig. 10 shows the variation of G_c as a function of temperature for 16 wt % carbon fibre specimen. G_c remains almost constant up to $-20°$ C, after which it rapidly increases. This trend can be attributed to the onset of the glass transition temperature ($\sim 0°$ C) of polypropylene.

4. Morphology–mechanical properties correlation

The procedure followed for specimen preparation using the brabender-mixing and mould compression technique seems to be effective. The moulded-specimen surfaces are smooth and do not contain pores or voids. Optical photographs shown in Fig. 11

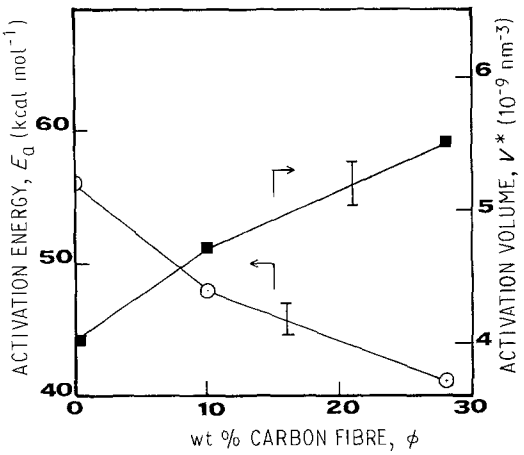

Figure 8 Variation of activation energy and activation volume as a function of carbon-fibre content.

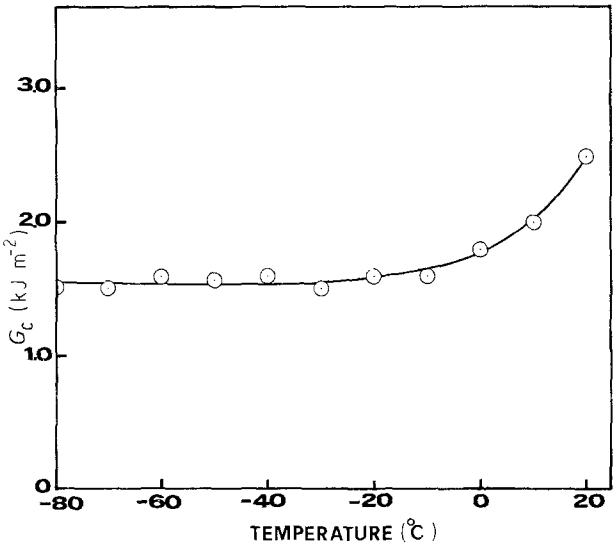

Figure 10 Dependence of critical strain energy release rate (G_c) on temperature for 16 wt % carbon fibre specimen.

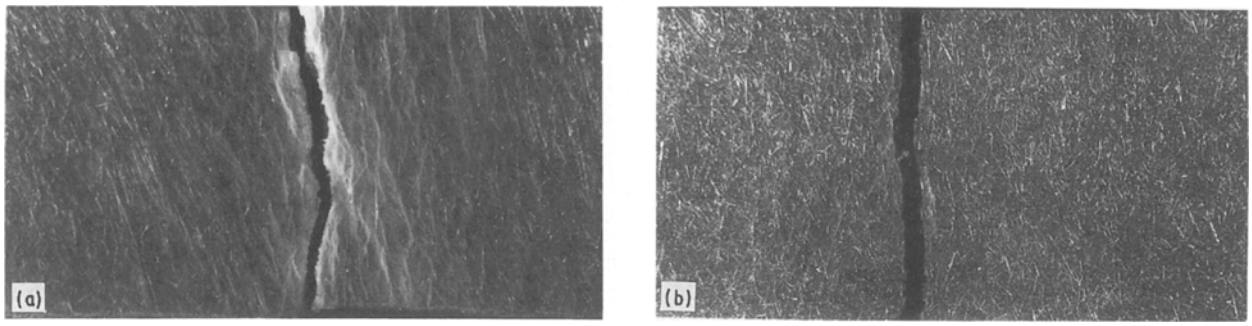

Figure 11 Optical photograph of specimens deformed by tensile tests: (a) 5 wt % fibre content (× 15); (b) 28 wt % fibre content (× 15).

exhibit surfaces with random fibre distribution at low and high carbon-fibre contents. Fig. 12 shows a scanning electron micrograph of the fractured surface of a specimen of 16 wt % carbon fibre content. The PP matrix surrounded the carbon fibre well, without voids around the fibres and in the matrix itself.

The mode of deformation of a composite in tension can be understood from the optical and scanning electron micrographs of Figs 11 and 12, respectively. The 5 wt % deformed specimen shown in Fig. 11 failed through a plastic deformation accompanied by wavy crazes, whiteness and transverse cracks without sharp edges. The 28 wt % specimen failed directly with a sharp-edge transverse crack. This mode of tensile deformation can be seen in the scanning electron micrographs of Fig. 13, where band shearing, whiteness and transverse cracks are clear in the 5 and 10 wt % deformed specimens (Figs 13a, b). Specimens with higher carbon-fibre content (Figs 13c, d) begin deformation with small transverse cracks, nucleate at carbon fibres, and finally fail with relatively straight edge transverse cracks.

These morphological observations could explain the decrease of the activation energy at yielding with increasing carbon-fibre content by taking into consideration the variation of the interfacial shear strength which is related to the yield stress as $\tau = \sigma_y/3^{1/2}$. The calculated value of τ (see Table I) decreases with ϕ; thus a smaller activation energy is required to overcome the potential barrier at the activated-rate yielding process. This argument is supported by the morphological characteristics seen in Fig. 13 where shear banding is observed only in deformed specimens of low carbon fibres. On the other hand, the activation volume, V^*, increases with carbon content because these fibres constitute entangled structural units and blocks with lower interfacial shear strength to convert from the unactivated state to the activated one under the applied external stress field.

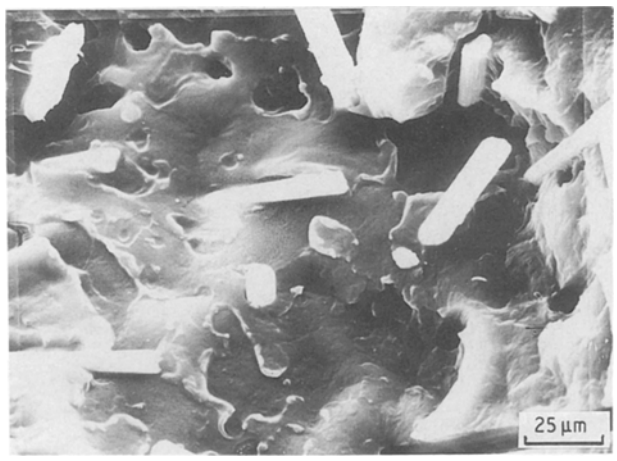

Figure 12 Scanning electron micrographs of 16 wt % carbon-fibre specimen fractured at room temperature.

The overall increase in the fracture toughness parameters with carbon-fibre content (Fig. 9) may be related to some morphological aspects of the composite material. The following observations were made from the SEM fractography.

1. For the 100% PP specimens, the features observed on the fracture surface (Fig. 14a) are spherulites with island-type structure where the plastic deformation near the crack tip took place by craze formation [21].
2. For specimens with low filler content (Fig. 14b) carbon fibres are well bonded to the PP matrix and a very small number of them are pulled out during the fracture process.
3. For specimens with high filler content (Figs 14c, d), even though a large number of carbon fibres are pulled out during fracture, there are some fibres still well bonded to the PP matrix.

Another important property required to improve the composite toughness is satisfied in that carbon fibres used as a filler in the present study have high strength, low modulus and high strain at the breaking load. The observed toughness behaviour of carbon-fibre composites was argued previously by a few workers such as Bader *et al.* [2] who concluded that the requirements for toughness improvement are good fibre–matrix bond, high fibre strength and strain at the breaking load and high fibre content. The results of the present study clearly show these factors exist and lead to better fracture toughness of the used high strength and low modulus carbon fibres. The increase of the fracture toughness or the resistance to impact of the fibre composite is attributed to composite delamination where the applied stress is suddenly

TABLE I

Material	Activation volume, V^* (nm^3)	Activation energy ($kcal\,mol^{-1}$)	Interfacial shear strength (MPa)
100% PP	3.99	56	20.6
10 wt % carbon fibre	4.65	48	19.2
28 wt % carbon fibre	5.47	41	16.9

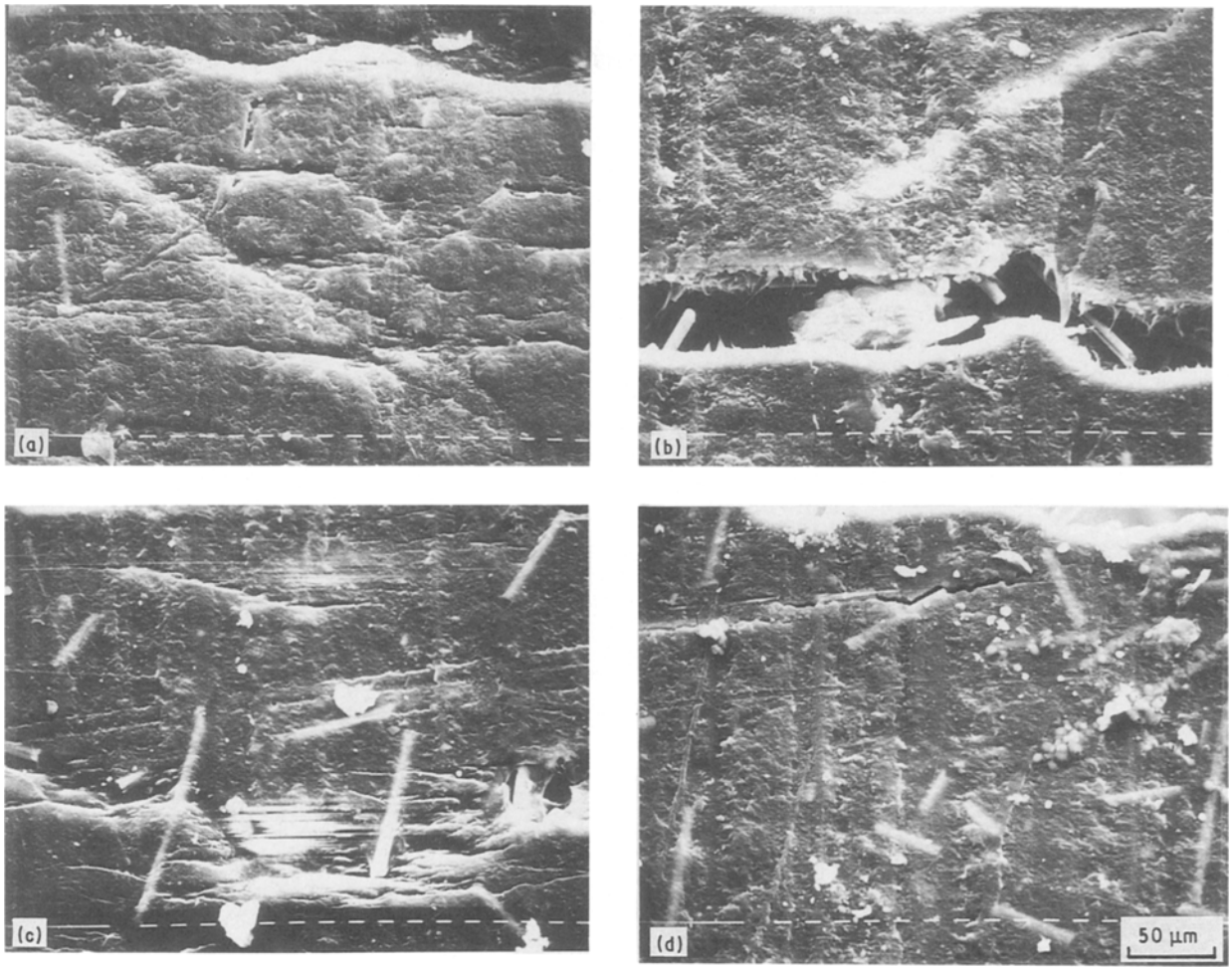

Figure 13 Scanning electron micrographs of composite specimens deformed under tensile tests: (a) 5% carbon fibres; (b) 10% carbon fibres; (c) 16% carbon fibres; (d) 28% carbon fibres.

accommodated and the impact energy is dispersed through the composite bulk. Thus, during fracture the amount of energy required to form voids and cracking at the fibre–matrix interface increases with increasing carbon-fibre networks supporting the applied loads, particularly in the crack-tip zone characterized by large plastic deformation. This requirement can be achieved by increasing the amount of carbon fibre in the polymeric matrix, resulting in a slow increase of the fracture parameters as shown in Fig. 9. For the purpose of comparison, it was pointed out by Friedrich and Karsch [22] that the particulate composite toughness is reduced by the addition of filler because the polymer fracture energy is considerable, due to plastic deformation, while the void formation and interfacial cracking between the polymer and spherical filler are usually small. So the fracture toughness behaviour of the fibre composite is different from that of the particulate composites, even though the polymer matrix is the same. One other point which is worthy of mention is that the scanning electron micrographs of the present fracture study do not exhibit a two-stage breakdown which frequently occurs consisting of compression buckling followed by tensile fibre rupture. The pull-out of the coated carbon fibre is observed at high fibre content in addition to some fibre shear banding, flaws and microcrazing phenomena which can be seen in the scanning electron micrograph of Fig. 14d.

5. Conclusions

Polypropylene-based composites reinforced with nickel-coated carbon fibres were prepared to study the variations of the tensile properties and fracture toughness with filler content over a range of temperature and strain rate. The measured physical quantities are correlated with the observed morphology of the deformed specimens in an attempt to understand the mechanism of composite breakdown and the role of fibre and matrix properties at the failure process. The following conclusions can be drawn from the results obtained.

1. The elastic modulus of such composites is increased by about two orders of magnitude and the tensile strength and strain to break are decreased.

2. The yield stress shows a temperature and strain-rate dependence. The calculated activation energy and activation volume of a rate-activated yielding process depend on the carbon-fibre content.

3. Yielding deformation takes place by shear banding, micrograzing and stretching effect of the polypropylene matrix at low fibre content; while at high fibre concentration the composite breaks in a brittle manner and pulling out of carbon fibres occurs.

4. The fracture behaviour of polypropylene is improved by addition of up to 28 wt % coated carbon fibres which form networks and structural interconnections in the matrix requiring a higher fracture energy with increasing fibre content.

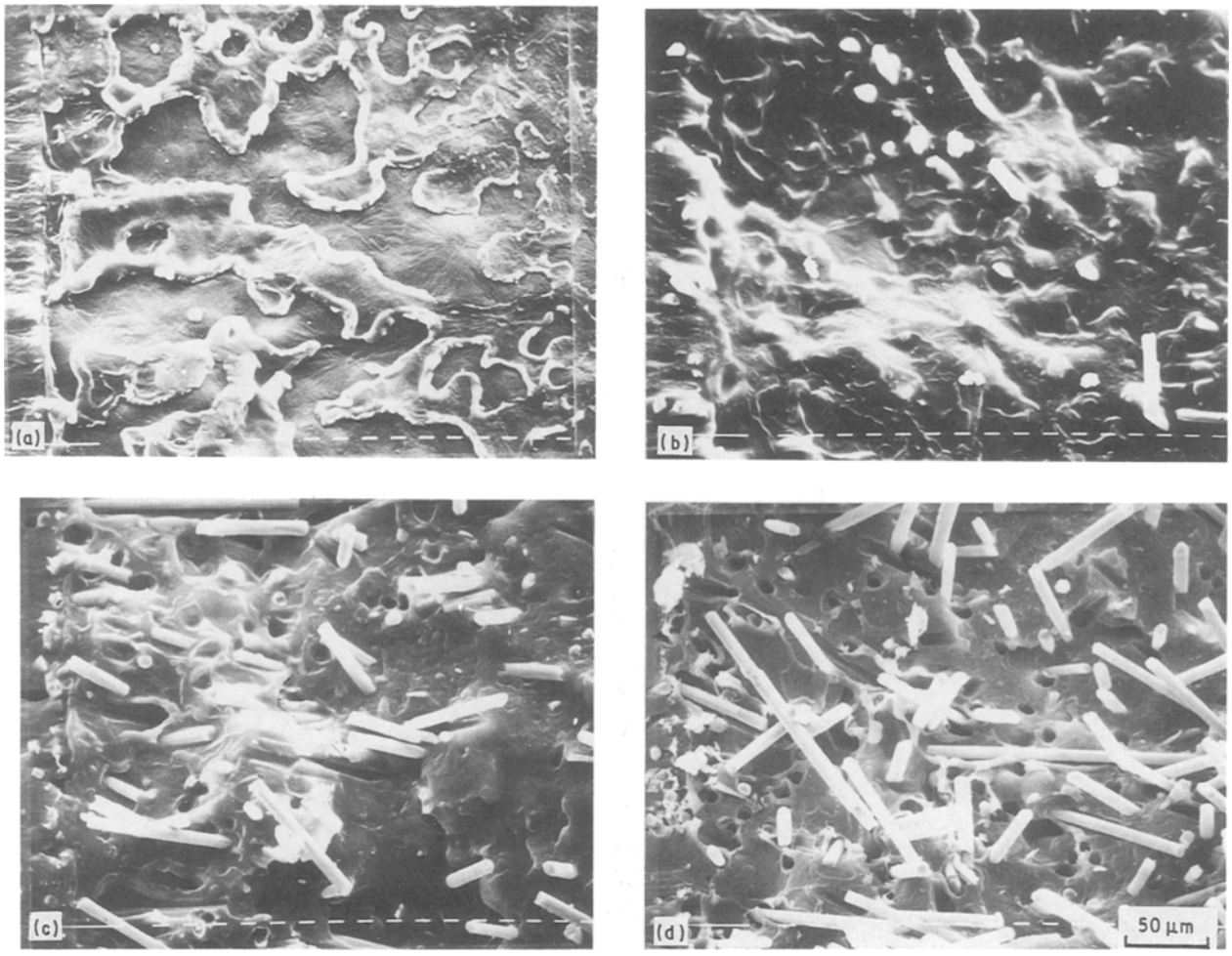

Figure 14 Scanning electron micrographs of composite specimens fractured under impact tests: (a) pure PP specimens; (b) 10% carbon fibres; (c) 16% carbon fibres; (d) 28% carbon fibres.

5. It was noticed, from the scanning electron micrographs, that the fracture process is associated with large plastic deformation occurring near the crack-tip region.

Acknowledgements

One of the authors is very grateful to both the International Centre for Theoretical Physics at Trieste, Italy, and the University of Jordan, Amman, for financial support. We thank Dr A. Abate for providing the carbon-fibre samples and Mr G. Narciso for typing the manuscript. This work has been partially supported by C.N.R. "Progetto Finelizzato Chimica Fine II".

References

1. G. LUBIN, "Handbook of Composites" (Von Nostrand, London, 1982).
2. R. M. GILL, "Carbon Fibers in Composite Materials" (The Plastics Institute, London, 1972).
3. M. A. MEYERS and O. T. INAL, "Frontiers in Materials Technologies" (Elsevier, Amsterdam, 1985) Ch. 12.
4. M. K. ABDELAZEEZ, M. S. AHMAD and A. M. ZIHLIF, *J. Mater. Sci.* **24** (1989) 1309–1315.
5. C. L. LHYMN and J. M. SCHULTZ, *Composites* **8** (1987) 287.
6. M. J. FOLKES and W. K. WONG, *Polymer* **28** (1987) 1309.
7. J. U. OTAIGBE and W. G. HARLAND, *J. Appl. Polym. Sci.* **36** (1988) 165.
8. WEN-YEN CHIANG and WEN-YEN YANG, *ibid.* **35** (1988) 807.
9. F. RAMSTEINER and R. THEYSOHN, *Composites* **15** (1984) 121.
10. M. AVELLA, E. MARTUSCELLI, C. SELLITTI and E. GARAGNANI, *J. Mater. Sci.* **22** (1987) 3185.
11. R. B. SEYMOUR and G. S. KIRSHENBAUM, "High Performance Polymers: Their Origin and Development" (Elsevier, New York, 1986).
12. L. A. GOETTLER, N.H.T.E.C. Proceedings, Florida, USA (1982) p. 151.
13. M. J. YASIN, I. EL-RIHAIL, M. S. AHMAD and A. M. ZIHLIF, *Mater. Sci. Engng* **86** (1987) 205.
14. P. D. COATS and I. M. WARD, *J. Mater. Sci.* **13** (1978) 1957.
15. L. FELDMAN, A. M. ZIHLIF, R. J. FARRIS and E. L. THOMAS, *ibid.* **22** (1987) 1199.
16. M. SUMITA, Y. TSUKUMO, K. MIYASAKA and K. ISHIKAWA, *ibid.* **18** (1983) 1758.
17. S. S. BHAGAWAN and S. K. DE, *Polym.-Plast. Technol. Engng* **27** (1) (1988) 37.
18. A. J. KINLOCH and R. I. YOUNG, "Fracture Behaviour of Polymers" (Applied Science, London, 1983).
19. R. GRECO and G. RAGOSTA, *Plastics Rubber Process. Applic.* **7** (1987) 163.
20. E. PLATI and J. G. WILLIAMS, *Polym. Engng Sci.* **15** (1975) 470.
21. R. GRECO and G. RAGOSTA, *J. Mater. Sci.* **23** (1988) 4180.
22. K. FRIEDRICH and U. A. KARSCH, *ibid.* **16** (1981) 2167.

Received 4 October 1988
and accepted 28 February 1989